Modification of the Secretion Pattern of Proteases, Inflammatory Mediators, and Extracellular Matrix Proteins by Human Aortic Valve is Key in Severe Aortic Stenosis*⒮

Gloria Alvarez-Llamas‡¶¶§§, Tatiana Martín-Rojas§¶¶, Fernando de la Cuesta§, Enrique Calvo¶, Felix Gil-Dones§, Veronica M. Dardé‖, Luis F. Lopez-Almodovar, Luis R. Padial**, Juan-Antonio Lopez¶, Fernando Vivanco‡‡‡‖‖, and Maria G. Barderas§‖‖**

One of the major challenges in cardiovascular medicine is to identify candidate biomarker proteins. Secretome analysis is particularly relevant in this search as it focuses on a subset of proteins released by a cell or tissue under certain conditions. The sample can be considered as a plasma subproteome and it provides a more direct approximation to the *in vivo* situation. Degenerative aortic stenosis is the most common worldwide cause of valve replacement. Using a proteomic analysis of the secretome from aortic stenosis valves we could identify candidate markers related to this pathology, which may facilitate early diagnosis and treatment. For this purpose, we have designed a method to validate the origin of secreted proteins, demonstrating their synthesis and release by the tissue and ruling out blood origin. The nLC-MS/MS analysis showed the labeling of 61 proteins, 82% of which incorporated the label in only one group. Western blot and selective reaction monitoring differential analysis, revealed a notable role of the extracellular matrix. Variation in particular proteins such as PEDF, cystatin and clusterin emphasizes the link between aortic stenosis and atherosclerosis. In particular, certain proteins variation in secretome levels correlates well, not only with label incorporation trend (only labeled in aortic stenosis group) but, more importantly, with alterations found in plasma from an independent cohort of samples, pointing to specific candidate markers to follow up in diagnosis, prognosis, and therapeutic intervention. *Molecular & Cellular Proteomics 12: 10.1074/mcp.M112.027425, 2426–2439, 2013.*

Degenerative aortic stenosis (AS)[1] is currently the most common cause of valve replacement in Western countries, and a significant increase in its prevalence is expected in the future because of increasing longevity (1). At the same time that our population age increases it can be expected that cardiac valve disease, and AS in particular, will increase in parallel. More and more, clinicians are seeing patients with symptomatic severe AS who are very advanced in age and have severe comorbidities or significant frailty, making operative intervention either impossible or of very high risk in the eyes of the cardiac surgeon. For this reason, the need of new diagnostic and prognostic methods, together with the urgent need of new drugs for therapy, has increased making a correct diagnosis in the early stages of the disease thereby reducing the cost burden to society. Several lines of evidence have demonstrated that degenerative AS is an active process in which inflammation plays a key role. As such, preventative approaches similar to those used in coronary artery disease (CAD) may be also applicable to AS (2, 3, 4, 5, 6). However, recent studies reported no reduction in later states of AS disease using statins, which significantly benefit patients with atherosclerosis (7, 8). Hence, further research is required to elucidate the pathogenic mechanism of this prevalent disease and to identify the similarities and differences in relation to atherosclerosis.

Proteomics has emerged as a particularly suitable platform for the nonbiased analysis of proteins involved in the pathogenesis of various diseases, such as AS (9, 10). This type of approach provided the basis for the development of biomarkers to detect patients at risk of developing degenerative AS. Plasma and serum have been the main source used in proteomic studies to identify candidate protein biomarkers, fol-

From the ‡Department of Immunology, IIS-Fundacion Jimenez Diaz, Madrid, Spain; §Department of Vascular Physiopathology, Hospital Nacional de Paraplejicos (HNP), SESCAM, Toledo, Spain; ¶Unidad de Proteomica, CNIC, Madrid, Spain; ‖Proteomic Unit, Hospital Nacional de Paraplejicos (HNP), SESCAM, Toledo, Spain; **Department of Cardiology, Hospital Virgen de la Salud, Toledo, Spain; ‡‡Department of Biochemistry and Molecular Biology I, Universidad Complutense, Madrid, Spain

lowed by tissue and cell samples. However, the use of plasma and serum is hampered by their complex nature and by the large dynamic range of protein concentrations, which may favor the detection of abundant proteins at the expense of those present at lower concentrations (11, 12). As such, the aortic valve secretome has emerged as an attractive target to further understand the AS pathogenic process. Tissue secretomes provide a more accurate model of the *in vivo* situation and, by minimizing serum contaminants, they facilitate the detection of low abundance proteins secreted into the blood (13).

In the present study, aortic valves from AS patients and nonaffected control subjects were cultured and the secretome analyzed by nLC-MS/MS. The addition of labeled amino acids to the culture media enabled the origin of the secreted proteins to be validated (truly secreted *versus* serum contaminants) and provided with information related to the dynamics of their synthesis and release from tissue.

<center>EXPERIMENTAL PROCEDURES</center>

Patient and Control Subjects Selection—Heart valves ($n = 20$) were obtained from AS patients of both sexes (55% male, 45% female), with an average age of 74 (± 4) years, presenting at the hospital with one or more of the cardinal AS symptoms (chest pain, dyspnea, syncope) and had undergone aortic valve replacement because of an echocardiography diagnosis of severe degenerative AS. All patients (100%) had hypertension, 50% suffered from hyperlipidemia and 60% from diabetes mellitus. Moreover, 60% of patients suffered coronary artery disease and surgery was indicated according to current practice guidelines. Neither antecedent of rheumatic fever, nor valvular morphologic changes consistent with rheumatic heart disease (*e.g.* typical mitral valve changes) were present in any patient. Patients with aortic regurgitation were also excluded in the study (Table I*A*). Control macroscopically normal valves ($n = 20$, Table I*B*) were obtained within 4 h from death from autopsies of subjects who had died from causes other than cardiovascular disease and who had no history of coronary artery disease or diabetes mellitus. Before resecting the valve, a cardiac surgeon explored it carefully. Valves with calcifications or cusp restriction were excluded as control cases. If inserted saline in aortic root remained in the closed valve, we ruled out significant regurgitation and we took these aortic valves as a control case. In all the cases, both stenotic and nonstenotic valves, the structure was 3-cuspid.

For a pilot selective reaction monitoring (SRM) validation analysis, peripheral blood samples ($n = 14$) were collected from AS patients and controls with comparable conditions; both cohorts had an average age of 74 years, were from both sexes (40% male, 60% female) and with analogous cardiovascular risks factors (100% hypertension, 60% diabetes, and 50% hyperlipidemia). AS plasma samples ($n = 7$) were obtained from patients who underwent aortic valve replacement because of severe degenerative AS. Plasma control samples ($n = 7$) were obtained from subjects with no apparent cardiovascular illness, and no history of coronary arterial disease. A greater cohort of 80 plasma samples (43 patients and 37 controls) was collected for a subsequent validation analysis using a nonbiased control population. This study was carried out in accordance with the recommendations of the Helsinki Declaration and it was approved by the ethics committee at the Hospital "Virgen de la Salud" (Toledo, Spain). Signed informed consent was obtained from all subjects or relatives in case of necropsies before their inclusion in the study. Clinical information is detailed in Supplementary Material.

Aortic Valve Tissue Culture—The aortic tissue was cultured as described previously (14), with minor modifications. Aortic valves with or without stenosis were transported from the operating room to the laboratory in PBS buffer at room temperature. The tissue was thoroughly washed three times with PBS supplemented with antibiotics and fungizone and washed twice more with 1640 Roswell Park Memorial Institute (RPMI) medium to eliminate serum contaminants. Samples were then transferred to a petri dish (Cell Star®), cut into pieces of about 1 mm³ and incubated separately at 37 °C in lysine-arginine free 1640 RPMI medium (Cell Culture Technologies Invitrus) supplemented with 5 mg/ml fungizone, 250 mg/ml amikazin, 2 mg/ml L-lysine 2HCl (U-^{13}C$_6$, 97–99%), and 10 mg/ml L-Arginine HCl (U-^{13}C$_6$, 97–98%: Cambridge Isotope Laboratories Inc., Andover, MA) in a humidified atmosphere of 5% CO_2. The culture medium was changed at 4 h and 8 h to eliminate serum contaminants and the tissue was incubated and collected for subsequent analysis at different time points (24 h, 48 h, 72 h, 96 h, and 120 h) to determine the point of maximum protein secretion. Collected media were stored at -80 °C until analysis (Fig. 1).

nLC-MS/MS Identification—Proteins released into the culture media by valve tissue (control or AS) were concentrated by ultrafiltration (Centriplus, 3-kDa cutoff, Millipore) and the protein concentration was determined by the Bradford method (Bradford assay, Bio-Rad, Hercules, CA). Subsequently, 25 μg of total sample protein were loaded onto SDS-PAGE and concentrated in a unique band that concentrated all the proteins in the sample, stained with Coomassie Brilliant Blue G-250 (PageBlue staining solution, Fermentas, Hanover, MD), excised in 15–20 small pieces and stored at 4 °C in ultrapure water for later analysis. Samples were subjected to reduction and alkylation before the in-gel digestion. Samples were in-solution digested by adding modified porcine trypsin (Promega) at a final ratio of 1:50 (trypsin-protein). Digestion proceeded overnight at 37 °C. After digestion, samples were vacuum-dried and finally dissolved in 1% acetic acid for LC-MS analysis. The resulting tryptic peptide mixtures were subjected to nano-liquid chromatography coupled to mass spectrometry for protein identification. Peptides were injected onto a C-18 reversed phase (RP) nano-column (100 μm I.D. and 12 cm, Mediterranea Sea, Teknokroma) and analyzed in a continuous acetonitrile gradient consisting of 0–50% B in 140 min, 50–90% B in 1 min (B = 95% acetonitrile, 0.5% acetic acid). A flow rate of 300 nL/min was used to elute peptides from the RP nano-column to an emitter nano-spray needle for real time ionization and peptide fragmentation on an LTQ-Orbitrap mass spectrometer (Thermo Fisher, San José, CA). An enhanced FT-resolution spectrum (resolution = 60000) followed by the MS/MS spectra from most intense five parent ions were analyzed along the chromatographic run (180 min). Dynamic exclusion was set at 0.5 min. For protein identification, tandem mass spectra were extracted and charge state deconvoluted by Proteome Discoverer 1.0 build 43 (Thermo Fisher Scientific). All MS/MS samples were analyzed using SEQUEST™ (Thermo Fisher Scientific, version 1.0.43.2) and by MASCOT™ program (Matrixscience, version 2.1). SEQUEST was set up to search human.fasta (1.0, 199762 entries). Mascot was set up to search a subset of SwissProt (51.6, 236102 entries). Both search engines were run assuming full trypsin digestion. Two missed cleavages were allowed and an error of 15 ppm or 0.8 Da was set for full MS or MS/MS spectra searches, respectively. All identifications were performed by Decoy database search for FDR analysis set at 0.05 by applying corresponding filters (Mascot Significance Threshold, and Score *versus* Charge state). Oxidation in M, phosphorylation in S, T, or Y, and SILAC+6 in K or R were selected as dynamic modifications.

Antibodies—The primary antibodies used to probe Western blots included: a mouse polyclonal antiserum against tenascin XB; monoclonal antibodies against clusterin, pentraxin 3 and gelsolin, all from

Table IA

A, Clinical characteristics of the patients with AS. Experiments carried out with every sample are indicated: secretome, western blot (WB), or selected reaction monitoring (SRM). (HTN) arterial hypertension

Patient num.	Age/Sex	HTN	Diabetes	Dyslipidemia	Discovery phase	WB	SRM
1	74/F	Yes	No	Yes	X		
2	73/M	Yes	Yes	No			X
3	68/M	Yes	No	Yes		X	
4	81/M	Yes	No	Yes		X	
5	69/M	Yes	Yes	Yes		X	
6	79/F	Yes	Yes	No			X
7	73/F	Yes	Yes	Yes		X	
8	77/M	Yes	No	No	X		
9	79/F	Yes	Yes	No			X
10	75/M	Yes	No	Yes		X	
11	74/M	Yes	Yes	Yes			X
12	74/F	Yes	Yes	No			X
13	79/F	Yes	Yes	No			X
14	79/F	Yes	yes	No			X
15	72/F	Yes	No	No		X	
16	63/M	yes	no	Yes			X
17	72/M	Yes	No	Yes			X
18	75/F	Yes	Yes	Yes			X
19	78/M	Yes	Yes	No		X	
20	74/M	Yes	Yes	No	X		
Mean	74 ± 4/45%F-55%M	100,00%	60,00%	50,00%			

Table IB

B, Clinical characteristics of control subjects. (COPD) Chronic obstructive pulmonary disease, (WB) Western blot, (SRM) selected reaction monitoring

Control num.	Age/Sex	Cause of the death	HTN	Discovery phase	WB	SRM
1	64/M	Bilateral acute bronchopneumonia	No	X		
2	51/F	Septic shock	Yes		X	
3	47/H	Sepsis	No			X
4	47/F	Bacterial pneumonia	No		X	
5	47/F	Carcinogenesis	No		X	
6	34/M	Acute Pancreatitis	Yes		X	
7	64/F	Bacterial Sepsis	No		X	
8	78/F	Aspiration bronchopneumonia	No			X
9	42/F	Lymphoma	No			X
10	67/M	Renal insufficiency	No			X
11	74/M	COPD	No	X		
12	87/F	Carcinoma	No			X
13	48/F	Pulmonary thromboembolism	No			X
14	55/M	Atypical pneumonia	No	X		
15	87/F	Cholelithiasis	No			X
16	76/M	Carcinoma	No		X	
17	80/F	Atrial fibrillation	Yes			X
18	49/F	Respiratory insufficiency	No			X
19	74/M	Septic shock	Yes		X	
20	77/F	COPD	Yes			X
Mean	69 ± 7/60%F-40%M		25,00%			

Abcam; and a monoclonal pigment epithelium-derived factor (PEDF) antibody (Lifespan Biosciences).

Western Blotting—Protein samples obtained from control and AS valve secretomes were resolved on 12% SDS-PAGE gels using a Bio-Rad Miniprotean II electrophoresis unit run at a constant current of 25 mA/gel for 1 h. Proteins were then transferred to a nitrocellulose membrane under constant voltage (15 V for 20 min) and the membranes were stained with Ponceau S to ensure equal protein loading

of the secretome samples. The membranes were then blocked with PBS-T containing 7.5% nonfat dry milk for 1 h (15), incubated overnight with the primary antibody in PBS-T containing 5% nonfat dry milk and subsequently incubated with the specific HRP-conjugated secondary antibody in the same solution.

SRM—Protein samples were reduced with 100 mM dithiothreitol (Sigma Aldrich) in 50 mM ammonium bicarbonate (99% purity; Scharlau) for 30 min at 37 °C, and alkylated for 20 min at room temperature

(RT) with 550 mM iodoacetamide (Sigma Aldrich) in 50 mM ammonium bicarbonate. The proteins were then digested in 50 mM ammonium bicarbonate, 15% acetonitrile (LC-MS grade, Scharlau) with sequencing grade modified porcine trypsin at a final concentration of 1:50 (trypsin/protein). After overnight digestion at 37 °C, 2% formic acid (99.5% purity, Sigma Aldrich) was added and the samples were cleaned with Pep-Clean spin columns (Pierce) according to the manufacturer's instructions. Tryptic digests were dried in speed-vac and resuspended in 2% acetonitrile, 2% formic acid (FA) before MS analysis. The LC-MS/MS system consisted of a TEMPO nano LC system (Applied Biosystems, Foster City, CA) combined with a nano LC Autosampler coupled to a modified triple quadrupole (4000QTRAP LC/MS/MS, Applied Biosystems). Three replicate injections (2 μg of protein in 4 μl) were performed per sample in the mobile phase A (2% ACN/98% water, 0.1% FA) at a flow rate of 10 μl/min for 5 min. Peptides were loaded onto a μ-Precolumn Cartridge (Acclaim Pep Map 100 C18, 5 μm, 100Å; 300 μm i.d. X 5 mm, LC Packings) to preconcentrate and desalt samples. Reversed-phase liquid chromatography (RPLC) was performed on a C18 column (Onyx Monolithic C18, 150 × 0.1 mm I.D., Phenomenex) in a gradient of phase A and phase B (98% ACN/2% water, 0.1% FA). The peptides were eluted at a flow rate of 300 nL/min in a continuous acetonitrile gradient: 2–15% B for 2 min, 15–50% B for 38 min, 50 to 90% B for 2 min and 90% B for 3 min. Both the TEMPO nano LC and 4000QTRAP system were controlled by Analyst Software v.1.4.2. The mass spectrometer was set to operate in positive ion mode with ion spray voltage of 2800V and a nanoflow interface heater temperature of 150 °C. The source and curtain gas were set to 20 and 10 psi respectively, and nitrogen was applied as both curtain and collision gases.

Theoretical SRM transitions were designed using MRMpilot software v1.1 (ABSciex), with the following settings: Enzyme = trypsin, missed cleavages = 0; modifications in peptide ≤ 3; charge states = +1 from 300 to 600 Da, +2 from 500 to 2000 Da, +3 from 900 to 3000 Da, +4 from 1600 to 4000 Da, +5 from 2400 to 10000 Da; studied modification = none; fixed modifications = carboxyamidomethylation; variable modifications = none; min. number of amino acids ≥ 5; max. number of amino acids ≤ 30; ignore multiple modification sites; 3 transitions per peptide (Table II). A pool containing a mixture of all the samples was digested as described previously and analyzed in the 4000QTrap using a MIDAS acquisition method that included the theoretical transitions. Transitions were selected when the three co-eluting peaks (corresponding to the three transitions of the same peptide) had a signal-to-noise ratio over 5 and the MS/MS data matched the theoretical spectrum for that peptide. Collision energy was optimized to obtain the maximum transmission efficiency and sensitivity for each SRM transition. A total of 24 transitions (3 per peptide) were monitored during an individual sample analysis. They were acquired at unit resolution in both Q1 and Q3, with dwell times of 50 ms resulting in cycle times of 1.2 s. The IntelliQuan algorithm included in Analyst 1.4.2 software was used to calculate the peptide abundance on the basis of peak areas after integration.

Pathway Analysis—Proteomics data were uploaded into the Ingenuity Pathways Analysis (IPA) (Ingenuity® Systems, www.ingenuity. com). Providing a list of GI accession numbers, biological networks were generated based on interactions between these selected genes and those stored in the Knowledge Base. Graphically, nodes correspond to genes and edges correspond to the biological relationships between them. IPA analysis computes a score for each network according to the fit of the user's set of significant genes. The significance value associated with functional analysis for a data set is a measurement of the likelihood that the association between a set of functional analysis molecules in the experiment and a given process or pathway is because of random chance.

TABLE II

List of proteins monitored by SRM analysis. Two peptides were selected for each protein monitored and three transitions for each peptide. Q1, m/z selected in first quadrupole. Q3, m/z selected in third quadrupole.

| Protein	Accession code	Accession n°	Peptide	Sequence	Q1 (charge)	Q3 (Fragment ion)		
						T1	T2	T3
Angiotensinogen	ANGT_HUMAN	P01019	ANGT_1	SLDFTELDVAAEK	719,36 (+2)	874,45 (y8)	975,50 (y9)	1122,57 (y10)
			ANGT_2	VLSALQAVQGLLVAQGR	862,01 (+2)	941,55 (y9)	1040,62 (y10)	1111,66 (y11)
EGF-containing fibulin-like extracellular matrix protein 1	FBLN3_HUMAN	Q12805	FBLN3_1	FSCMCPQGYQVVR	816,36 (+2)	721,4 (y6)	946,51 (y8)	1106,54 (y9)
			FBLN3_2	NPCQDPYILTPENR	858,9 (+2)	1102,59 (y9)	1217,62 (y10)	1345,67 (y11)
Gelsolin	GELS_HUMAN	P06396	GELS_1	AGALNSNDAFVLK	660,35 (+2)	806,44 (y7)	893,47 (y8)	1007,52 (y9)
			GELS_2	QTQVSVLPEGGETPLFK	915,49 (+2)	1074,55 (y10)	1187,63 (y11)	1286,7 (y12)
Prostaglandin D2 synthase	PTGDS_HUMAN	P41222	PTGDS_1	TMLLQPAGSLGSYSYR	872,44 (+2)	989,47 (y9)	1157,56 (y11)	1285,62 (y12)
			PTGDS_2	AQGFTEDTIVFLPQTDK	955,48 (+2)	1060,6 (y9)	1276,68 (y11)	1405,72 (y12)
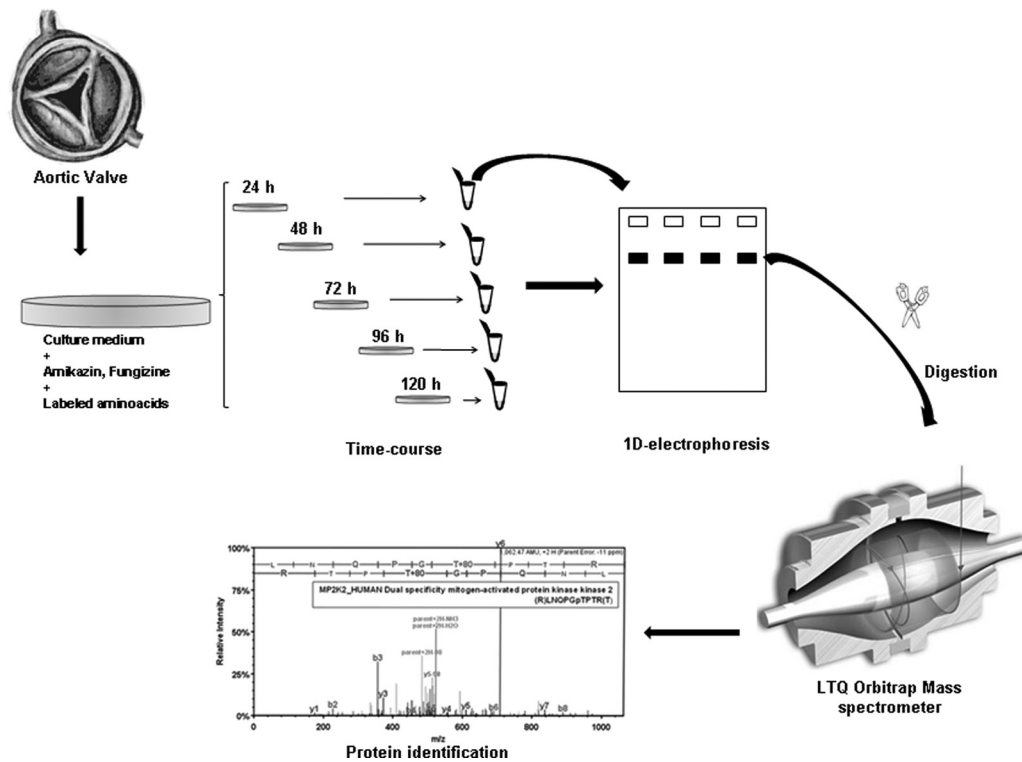
FIG. 1. **Secretome from aortic valves and the proteomic analysis workflow.** Schematic representation of the workflow for aortic valve tissue culture and the subsequent proteomic analysis, showing secretome collection, protein extraction and LC-MS/MS analysis.

Statistical Analysis—Western blot bands were measured using a GS-800 Calibrated Densitometer (Bio-Rad) and the values obtained analyzed using the statistical software packages SPSS 13.0 and GraphPAD Instat (GraphPAD software). A Kolmogorov-Smirnov test was applied to evaluate normal distribution of the population analyzed. When normal distribution was demonstrated, a Levene test for homogeneity of variance was performed and the Student t test was used to compare band intensities and SRM peak areas, selecting adequate p value in view of homogeneity results. For populations with no normal distribution, the nonparametric Mann-Whitney U test was used. Right tailed Fischer Exact Test was applied for IPA analysis. For all tests, statistical significance was accepted when $p < 0.05$. All LC-MS/MS identifications were performed by Decoy database search for FDR analysis set at 0.05 by applying corresponding filters (Mascot Significance Threshold, and Score *versus* Charge state).

RESULTS

Secretome Characterization: Metabolic Labeling of Secreted Proteins—The secretome from human control and AS valves from three individuals per group (3 patients, 3 controls) was obtained and the labeled proteins detected were investigated (Fig. 1). The maximum number of labeled proteins from both pathological and healthy valves was obtained at 96 h (Fig. 2*A*), when 248 proteins were unambiguously identified in total, labeled or not. Among these, 61 proteins were labeled in at least one of the three secretome replicates from either of the two groups (control or patient), 50 in AS and 23 in control aortic valves (Fig. 2*B*). Twelve proteins of the 61 were secreted by both AS and control valves. All the labeled proteins were analyzed using the SecretomeP software (16) to

predict them as being secreted: the presence of a signal peptide indicated secretion by the classical pathway and a NN-score of over 0.5, in the absence of a signal peptide, indicated nonclassical secreted proteins. Of the 61 proteins, 36 contained a signal peptide and 9 proteins were found to be nonclassically secreted. Among the 17 proteins not predicted to be secreted by Secretome P, 5 had been previously detected in serum/plasma (according to the Human Protein Reference Database: www.hprd.org).

The labeled proteins were classified into six different groups based on their molecular function (*UniprotKB database*): extracellular matrix constituents (ECM)/cytoskeletal, immune response, degradation, transport/metabolic processes, regulatory function, and other (Fig. 2*B*). Pathway analysis on proteomics data from Table III shows "Cellular Movement, Connective Tissue Disorders, Cardiovascular System Development and Function" as the main associated functional network (see Fig. 3). "Cardiovascular System Development and Function" and "Tissue Development" were the most significant functions related to Physiological System Development, with 18 and 23 proteins from the data set involved, respectively. Additional data can be found in supplemental material and in ftp://PASS00237:BE5743t@ftp.peptideatlas.org/.

Secretion Pattern in Aortic Stenosis—Of the 61 labeled proteins, 50 (82%) incorporated the label in only one of the two groups (control = 11 and AS = 38: Table III). These proteins deserve particular attention as they represent poten-
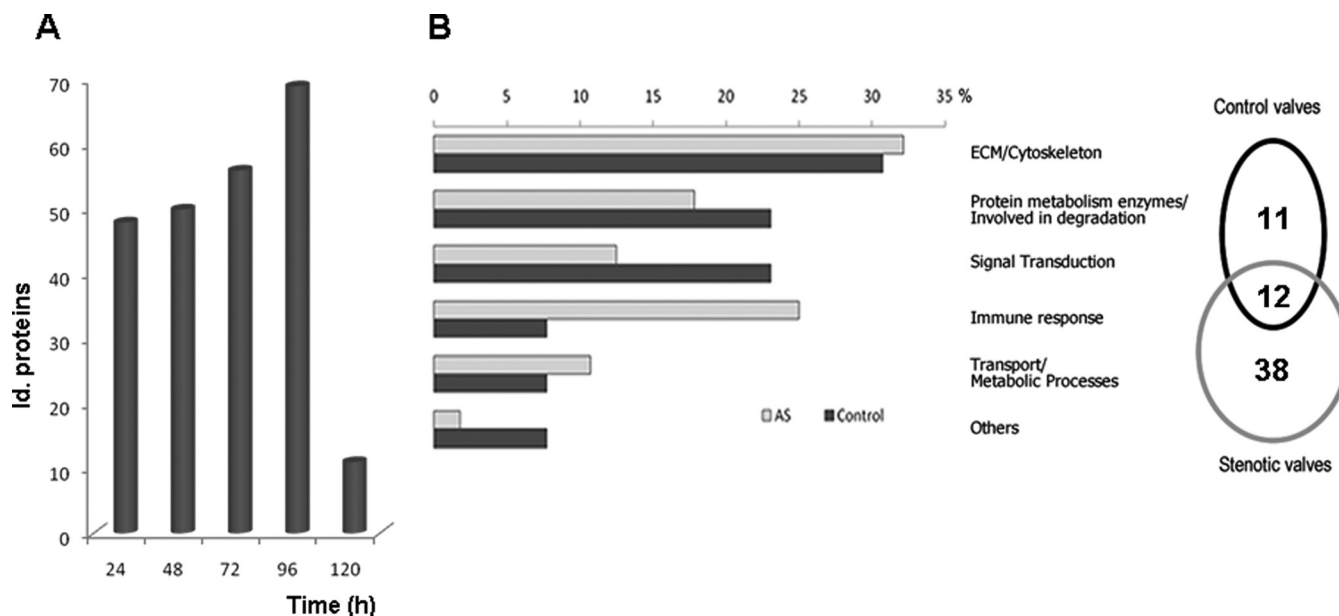
FIG. 2. **Time course and functional classification.** *A*, Total number of identified labeled proteins at every time point including all replicates for both controls and patients. *B*, Sixty-one proteins were labeled in at least one of the three secretome replicates of either of the two groups (control or patient) after 96 h in culture. Of these proteins, 50 were observed in aortic stenosis (AS) valves and 23 in control valves. The secreted and labeled proteins were classified into six different groups based on their molecular function.

tial diagnostic and therapeutic targets, given that they reflect the main differences observed between affected and healthy tissue at the protein level. We analyzed additional secretome samples ($n = 4$ per group for each analysis by Western blot and $n = 10$ per group by SRM) to those used in the discovery phase, from both control and AS groups.

Western Blot Analyses—A group of five proteins was analyzed in Western blot analysis (Fig. 4), demonstrating that clusterin (Fig. 4*A*) and tenascin XB (Fig. 4*B*) were downregulated in AS valve secretome samples when compared with the control samples ($p = 0.0224$ and $p = 0.0002$, respectively). By contrast, the expression of gelsolin (Fig. 4*C*), pentraxin 3 (PTX3, Fig. 4*D*) and pigment epithelium-derived factor (Fig. 4*E*) was up-regulated in AS secretome valves ($p = 0.0112$, $p < 0.0001$, $p = 0.0002$, respectively).

SRM Analyses—Secretomes obtained from an independent group of aortic valve samples ($n = 10$ controls, $n = 10$ AS patients) were analyzed by SRM. In particular, four proteins that incorporated the label in only one of the two groups were measured. In all cases, the two peptides measured for each protein were found to differ significantly their expression (Fig. 5). This was observed for both angiotensinogen peptides (Fig. 5*A*, $p < 0.0001$), for EGF-containing fibulin-like extracellular matrix protein 1 (Fig. 5*B*, $p = 0.0362$ peptide1 and $p = 0.0349$ peptide 2) and for gelsolin (Fig. 5*C*, $p = 0.0197$ peptide 1 and $p < 0.0001$ peptide 2). The expression of all of these proteins was up-regulated in AS *versus* control secretomes. In contrast, prostaglandin-D2 synthase (Fig. 5*D*, $p = 0.0084$ peptide 1 and $p < 0.0001$ peptide 2) was down-regulated in AS *versus* control secretomes (Fig. 5).

Reflection in Plasma—In an independent cohort of plasma samples ($n = 7$ controls, and $n = 7$ AS patiens) matched by sex, age, and AS risk factors (hypertension, diabetes, and dyslipidemia), three proteins were analyzed by SRM: clusterin ($p = 0.0053$), gelsolin ($p = 0.0253$), and prostaglandin D2 synthase ($p = 0.0236$) (see Supplementary Figures). In this first pilot study, differential trends observed by WB or SRM in plasma corroborated previous findings in secretome samples and allowed excluding sex, age, and AS risk factor bias. More importantly, results suggest that some proteins found differentially expressed in the secretome analyses could be validated in patients' plasma. ROC curves calculated for the three proteins showed the best results for gelsolin (area under the curve, AUC = 0.950) (see Supplementary Figures). Among all proteins tested in secretome samples, gelsolin showed the same trend (increased in AS group) independently of the strategy used for validation and in all the approaches tested (WB and SRM). Interestingly, this protein followed the opposite trend in the secretome from atherosclerotic coronary arteries (13). For all these reasons and considering the limited knowledge about common and specific operating mechanisms in AS and atherosclerosis pathologies, we further validate gelsolin response in a new, wider and independent cohort of samples. To prove the potential of this protein as marker of AS, gelsolin was comparatively analyzed by SRM in a cohort of 80 plasmas (43 patients and 37 controls), finding again that plasma levels increased in patients' cohort and corroborating previous findings (Fig. 6*A*). ROC curve (AUC = 0.950) is shown in Fig. 6*B*. The two peptides measured with three transitions per peptide gave significant variation (p val-

TABLE III

Proteins labelled in at least one replicate from either of the two groups. P//C: Number of AS patients (P) or controls (C). Sec, Secretion pathway of the proteins found in plasma, according to the secretome P software and the Human Protein reference database. NS: no secreted, CP: secreted by classical pathway, NCP: secreted by nonclassical pathway, BL: detected in serum or plasma

P//C	Sec.	Accession	Gen name	Protein name	Function
3//2	NS, BL	GI:53791223	FINC	Fibronectin 1	Extracellular matrix structural constituent
3//0	CP	GI:220125	TIMP	Tissue inhibitor of metalloproteinases	Alloendopeptidase inhibitor activity
2//1	CP	GI:4502403	BGN	Biglycan preproprotein	Extracellular matrix structural constituent
3//1	NS	GI:30851190	CO6A1	Collagen, type VI, alpha 1 precursor	Extracellular matrix structural constituent/cell adhesion
3//0	NS	GI:179716	CO7	Complement C7	Extracellular matrix structural constituent/cell adhesion
1//0	NS	GI:2065167	COL14A1	Collagen, type XIV	Extracellular matrix structural constituent/cell adhesion
1//0	NS	GI:296439507	CO1A2	Prepro-alpha2(I) collagen	Extracellular matrix structural constituent/cell adhesion
3//3	CP	GI:11342666	MMP2	Matrix metalloproteinase 2 (Gelatinase A)	Endopeptidase activity
2//0	CP	GI:119226208	PTGDS	Prostaglandin D2 synthase 21kDa	Transporter activity
3//0	CP	GI:144226251	CHI3L1	Chitinase-3-like protein 1	Chitinase activity
3//0	CP	GI:40217843	COMP	Cartilage oligomeric matrix protein	Extracellular matrix structural constituent
1//0	NS	GI:71773110	APOB	Apolipoprotein B-100	Transporter activity
1//0	NS	GI:311254603	CHI3L2	Chitinase 3-like 2 isoform a	Chitinase activity
1//0	NS	GI:4502693	CD9	CD9 antigen (27 kDa diphtheria toxin receptor-associated)	Immune response: platelet activation and aggregation
1//2	CP	GI:4505047	LUM	Lumican precursor	Extracellular matrix structural constituent
2//2	CP	GI:75075054	CERU	Ceruloplasmin precursor	Chaperone/Ferroxidase enzyme
1//0	CP	GI:4506141	HTRA1	Serine protease HtrA	Serine-type endopeptidase activity
2//0	CP	GI:11118375	ANGT	Angiotensinogen (serpin peptidase inhibitor)	Acetyltransferase stimulator activity
1//0	CP	GI:189580	PAI1	Plasminogen activator inhibitor type 1	Coagulation
1//0	CP	GI:119592657	LENG9	Leukocyte receptor cluster (LRC) member 9	Receptor activity/Immune response
1//0	NCP	GI:19923830	PBIP1	Pre-B-cell leukemia transcription factor interacting protein 1	transcription corepressor activity
1//0	NCP	GI:207101417	CAR82030	Unnamed protein product Fab	Unknown
1//0	NCP	GI:7438711	JE0242	Ig kappa chain NIG26 precursor	Immune response
2//0	NCP	GI:229601	IGHG1	Ig G1 H	Immune response
1//0	NCP	GI:229585	IGHA1	Ig A1	Immune response
1//0	CP	GI:189778	PEDF	Pigment epithelial-derived factor	Potent inhibitor of angiogenesis
2//2	NS	GI:40317626	TSP1	Thrombospondin 1 precursor	Collagen V binding
2//0	CP	GI:181192	CATB	Preprocathepsin B	Cysteine protease
1//0	CP	GI:4504165	GELS	Gelsolin isoform a	Actin binding
1//0	CP	GI:50659080	AACT	Alpha-1-antichymotrypsin	Immune response
2//0	CP	GI:73858570	IC1	Plasma protease (C1) inhibitor	Protease inhibitor
1//0	CP	GI:5901956	FSTL3	Follistatin-related protein 1 precursor	BMP signaling pathway
1//0	NS, BL	GI:119631316	CO3A1	Collagen, type III	Extracellular matrix structural constituent
1//0	NCP	GI:53759113	B4GT2	Beta1,4-galactosyltransferase-2	Metabolic process: N-acetyllactosamine synthase activity
2//2	NCP	GI:23396609	IBP7	Insulin-like growth factor binding protein 7	Signaling/regulatory function
1//0	NS	GI:51477704	SMRC1	SWI/SNF-related matrix-associated actin-dependent regulator	Transcription regulator
1//0	NS	GI:11320820	SPON1	VSGP/F-spondin	Extracellular matrix structural constituent
1//0	CP	GI:1709663	PLTP	Phospholipid transfer protein	Lipid transport, lipid binding
1//0	CP	GI:15072400	FBLN3	EGF-containing fibulin-like extracellular matrix protein 1	Extracellular matrix structural constituent
1//1	CP	GI:46981969	PIG35	Proliferation-inducing protein 35	Negative regulation of angiogenesis
1//0	CP	GI:77176698	PTX3	Pentraxin-related protein PTX3	Imflamatory response
1//1	CP	GI:10834984	IL6	Interleukin 6 (interferon, beta 2)	Immune defense
1//0	NCP	GI:119596921	PCOC2	Procollagen C-endopeptidase enhancer	Extracellular matrix structural constituent
1//0	CP	GI:4261568	CATD	Cathepsin D	Involved in degradation: proteolysis
1//1	CP	GI:41393602	C1S	Complement subcomponent C1s	Immune response
1//0	CP	GI:4503107	CYTC	Cystatin C precursor	Involved in degradation: cysteine-type endopeptidase inhibitor activity
3//0	NS, BL	GI:62088774	COL1A1	Collagen alpha-1 chain precursor	Extracellular matrix structural constituent

TABLE III—*continued*

P//C	Sec.	Accession	Gen name	Protein name	Function
1//0	CP	GI:15079241	IBP5	Insulin-like growth factor binding protein 5 protease	Signaling/regulatory function
1//0	CP	GI:29788996	PON3	Beta-alanine/gamma-aminobutyrate-H+ symporter	Involved in degradation: arylesterase activity
2//3	CP	GI:27373753	CLUS	Clusterin precursor	Apoptosis
0//1	NS, BL	GI:120537932	TENX	Tenascin XB	Extracellular matrix structural constituent/Cell adhesion
0//1	CP	GI:4504991	NFKB2	Leukemia inhibitory factor precursor	Transcription regulator
0//1	CP	GI:134218	SAP	Saposin precursor	Lipid transport
0//2	CP	GI:115298678	CO3	Complement C3 precursor	Immune response
0//1	NCP	GI:190359980	PPR3E	Protein phosphatase 1 regulatory subunit	Glycogen metabolic process
0//1	NS, BL	GI:6648082	PYGL	Glycogen phosphorylase	Energy pathways, phosphorylase activity
0//1	CP	GI:47678717	TIMP3	Matrix metalloproteinase 3, preproprotein	Involved in degradation: metalloendopeptidase inhibitor activity
0//1	CP	GI:79749430	FREM2	Fras1 related extracellular matrix protein 2	Extracellular matrix protein
0//2	CP	GI:1209010	TIMP1	Metalloproteinase tissue inhibitor 1	Involved in degradation: metalloendopeptidase inhibitor activity
0//2	CP	GI:66932947	A2MG	Alpha-2-macroglobulin precursor	Proteinase activity
0//1	NS	GI:83321247	KIR3DL3	KIR antigen	Receptor activity

ues for peptide 1: 0.035, 0.00088, and 0.0106; *p* values for peptide 2: 0.0029, 0.0109, and 0.0052).

DISCUSSION

To our knowledge, this represents the first exhaustive proteomic analysis of the aortic valve secretome. We conducted an in-depth analysis of the secretome of aortic valves to obtain a data-set of potential AS biomarkers and to shed light on the underlying pathophysiological mechanisms. Because of the high social cost derived from AS healthcare, the establishment of diagnostic and prognostic biomarkers to allow early detection of the disease, as well as therapeutic targets, is highly necessary. By proteomic approaches we may be able to diagnose the disease even before traditional methods (ecography) do and even before macroscopic changes produced in the aortic valve are observed. Indeed, it is important to note that it is at these initial phases of the disease when most effect could be expected from new drug action. Additionally, novel tools for early diagnosis will avoid the high morbidity and mortality risks associated with surgery and acting in time may provide a solution for those patients who cannot have surgery.

The metabolic labeling approach used allowed us to differentiate between proteins synthesized by the tissue (labeled) and contaminating proteins from the blood that remain unlabeled (14). The major problem when analyzing tissue secretome is the presence of plasma contaminants, which should be minimized using an optimized culture protocol developed for this purpose. Proteins that incorporate the label and contain a signal peptide (classical pathway) or, if not containing it, had a NN-score of over 0.5 according to Secretome P software (nonclassical pathway) were considered to be genuinely secreted by aortic valve tissue, because incorporation of the label by a protein does not necessarily imply "intentional" secretion. However, once synthesized by the tissue, the release of nonsecreted protein into the media could be attributed to damage-induced tissue leakage, which may be a direct consequence of the pathology under study. This approach is here applied for the first time to human valvular tissue. Hence, valvular tissue showed a dynamic nature as proven by the label incorporation in a significant number of proteins. Based on our previous experiments with other tissues, labeling efficiency depends on the analyzed tissue, in some cases being insignificant (data not shown). At the optimum time point (96 h), 248 unique proteins were detected in the secretome of control and AS aortic valves, with 23 and 50 proteins incorporating the metabolic label in control and AS valves, respectively, most of which (82%) were only labeled in one of the two groups. In this sense, differences in labeling incorporation somehow reflect tissue activity and, thus, these proteins may better discriminate between pathological and healthy conditions, having a significant role in AS development. The functional classification of the selected secreted proteins indicated that a significant number were ECM proteins. This protein type serves as a structural support, maintaining the cell architecture, and these proteins play a pivotal role in both morphogenesis and tissue regeneration through ECM remodeling (17). ECM proteins include collagens, noncollagenous glycoproteins, and proteoglycans. Organization of these components into a fibrillar framework provides the mechanical strength and elasticity required for cell adhesion and migration. The alterations in ECM composition observed may therefore indicate active tissue remodeling with a loss of elasticity in the aortic valve. From this group, differences in label incorporation and secretion observed by LC-MS/MS for tenascin XB, EGF-containing fibulin-1, gelsolin, and pigment epithelium derived factor proteins correlated well with protein
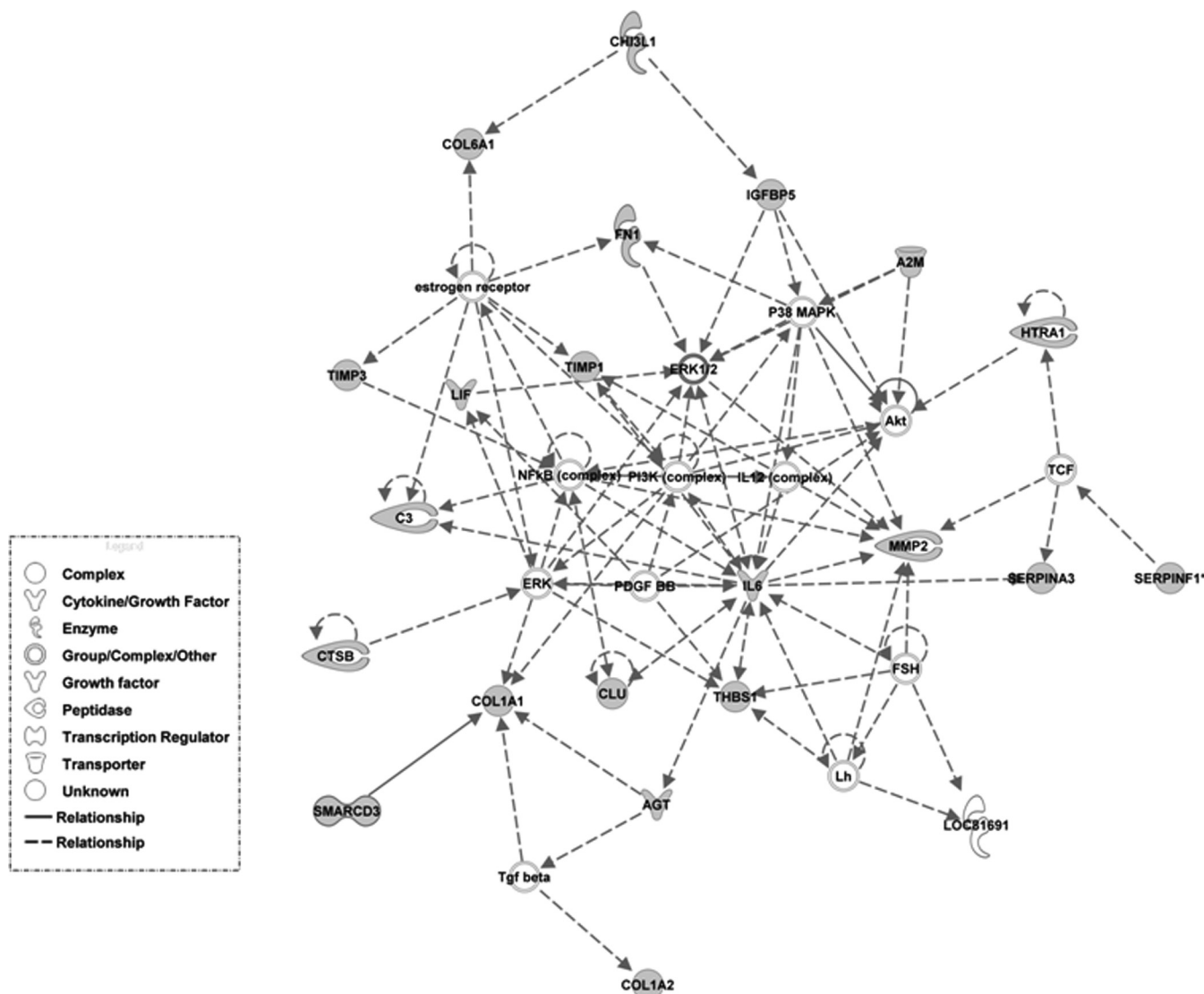
FIG. 3. **Top network of the sub-set of 61 proteins found labeled in the secretome of either of the two groups revealed by Ingenuity Pathways Analysis (IPA).** Biological networks were generated based on the interactions between these proteins and those stored in the IPA Knowledge Base. Graphically, nodes correspond to proteins and edges correspond to the biological relationships between them.

abundance validation analyses. Additionally, angiotensinogen, clusterin, and pentraxin 3 trends also correlate.

The decrease in tenascin XB in patients could be attributed to a functional similarity with tenascin C, with which it shares a common FNIII domain, several repeats of which are found in tenascin XB. Tenascin C is expressed in the cardiac vasculature, where it is implicated in local vascular remodelling (6). If its secretion pattern is modified in AS compared with a healthy status, the interactions between tenascin-C and both endothelial cells and endothelial precursor cells (EPCs) will also be altered. In this context, and considering the similarity between tenascin C and tenascin XB, this protein and its interactions may represent a novel target to follow disease and, in particular, to act on in order to favor the enhancement of vascular repair mechanisms, known to be down-regulated

with age and in pathological conditions (18). Importantly, decreased tenascin XB levels are associated with various problems of mitral and tricuspid valves (16). Furthermore, the decrease in tenascin XB seen in Ehler Danlos syndrome increase the probability of aortic aneurisms (19).

We detected an increase in EGF-containing fibulin-like protein secretion in AS valves. Fibulins are abundant in dynamic connective tissues associated to arteries, lung, skin, and ligaments (20), where they provide elastic recoil and resilience. Fibulins also provide an important adhesion template for cells, regulating growth factor availability (21) and participating in diverse supramolecular structures (22). The increased fibulin secretion observed in AS tissue culture suggests a loss of elasticity in the tissue, which together with other factors and proteins, may promote its calcification. Another fibulin, fibu-
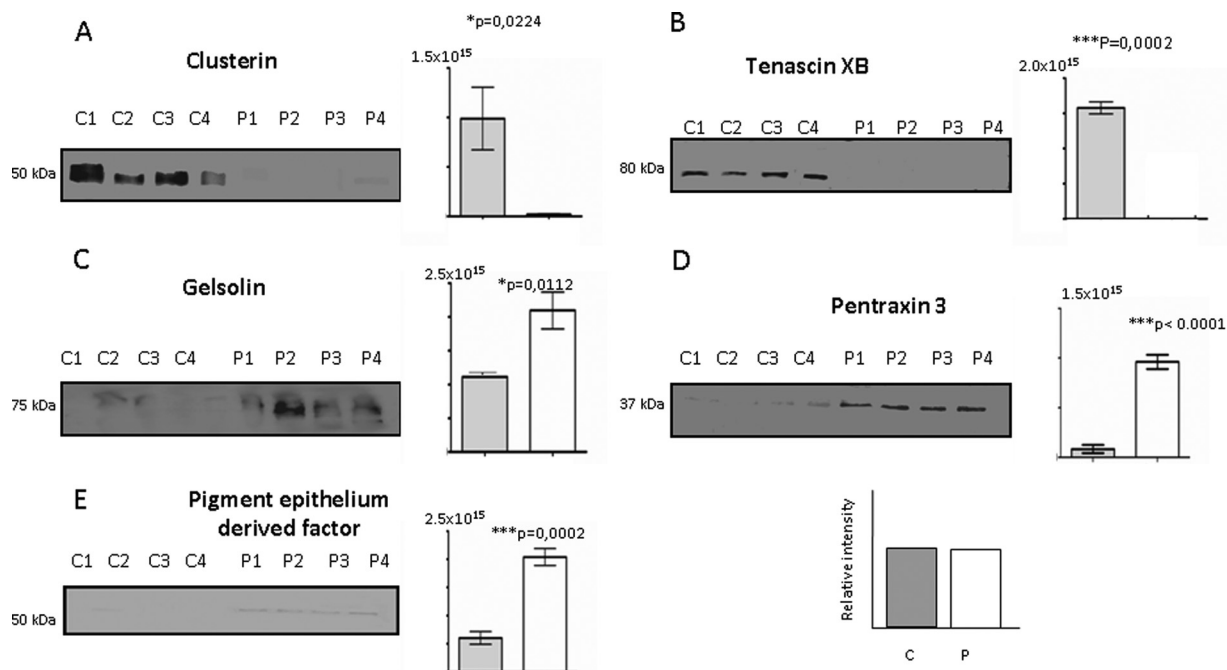
FIG. 4. **Western blot validation of the labeled proteins.** (*A*) Clusterin (50 kDa) and (*B*) tenascin XB (80 kDa) levels decreased in AS cultures (P1 to P4) with respect the controls (C1 to C4). In contrast (*C*) gelsolin (75 kDa), (*D*) pentraxin 3 (37kDa), and (*E*) pigment epithelium derived factor (PDEF, 50 kDa) augmented in AS cultures when compared with controls. Corresponding p values (Student's t test) for each protein analyzed are shown. $* = p < 0.05$, $** = p < 0.01$, $*** = p < 0.001$.

lin-5 has also been implicated in severe hereditary connective tissue diseases such as supravalvular aortic stenosis (8).

Gelsolin is an actin binding protein with multiple regulatory activities that include cytoskeletal remodeling and ion channel regulation (23, 24). Increased gelsolin expression has been reported in failing hearts and it may contribute to the perturbation of thin filament organization (25, 26). Gelsolin has also been implicated in the cardiac remodeling triggered by ischemic heart disease, as described in both animal models of heart failure (15) and human hearts (27). We observed an increase in gelsolin expression in AS valves, which suggests that a similar remodeling process may occur in AS. Indeed, as a consequence of endothelial damage (28), endothelial cells are continuously exposed to mechanical forces generated by blood flow (29), and unidirectional shear stress increases the expression of proteins involved in adaptive processes to reduce flow-induced endothelium damage (18, 30). Moreover, the permanent decline in contractile function may also affect the expression of cytoskeletal proteins (31).

Pigment epithelium derived factor (PEDF), a glycoprotein of the serine protease inhibitor super-family, is a highly effective inhibitor of angiogenesis in cell culture and animal models (32, 33, 34), and it exerts antioxidant (35) and antithrombotic (36) effects. As oxidative stress is associated with an increase in cardiovascular risk (37), an increase in PEDF may protect cells from the negative effects of oxidative stress. Recently, an extensive study to analyze coronary plaques using a shotgun proteomic approach described increases in PEDF in atherosclerotic plaques (38). Hence, a link between atherosclerosis and aortic stenosis disease in relation to this concrete pathway may exist, which merits further investigation.

Angiotensinogen, clusterin, and pentraxin 3 differences found in label incorporation and secretion by LC-MS/MS were also correspondent with protein abundance validation analyses. T lymphocytes and macrophages infiltrate the endothelium and release cytokines, which in turn induce cellular proliferation of valve fibroblasts and extracellular matrix remodeling (39). This process results in increased secretion of proteins such as angiotensinogen (AGT), which exert wide-ranging effects on the endothelium and vascular smooth muscle such as vasoconstriction (40), because of its processing to angiotensin II peptide, which contributes to hypertension (21), and activation of endothelial proliferation (41). The increased secretion of AGT in AS valves may explain the thickening of the aortic valve due to its proliferative effect in valve fibroblasts, which precludes valve opening (5). Regarding prostaglandin D2 synthase (PGD2) protein, it inhibits platelet aggregation and induces vasodilatation (42). PGD2 is widely distributed in the peripheral tissues and localized in antigen-presenting cells and mast cells (43), from which it is released as an allergic and inflammatory mediator (44). We detected a decrease in PGD2 secretion in AS valves, implying a more limited vasodilatatory effect, which may contribute to the vasoconstriction of aortic stenosis valves provoked at the cellular
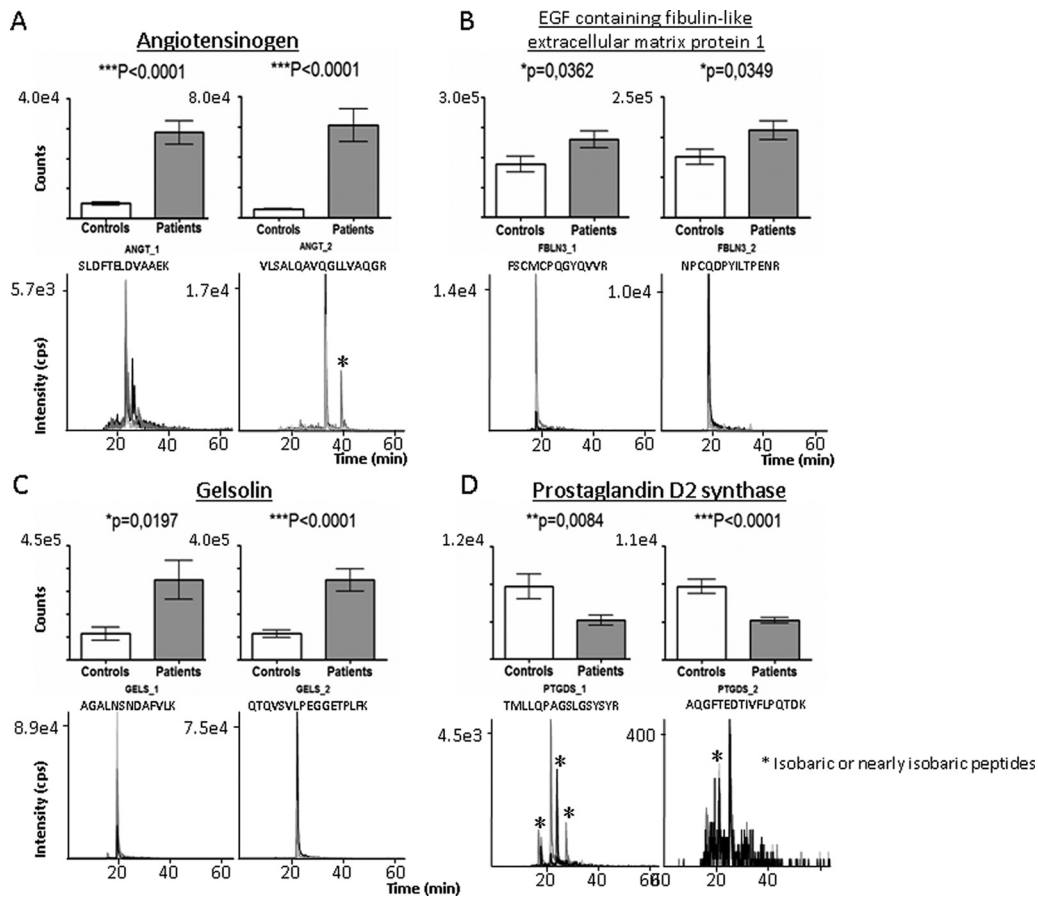
FIG. 5. **Validation of labeled proteins by SRM analysis.** Graphical representation of the abundance (*upper* panels) and representative extracted ion chromatograms (*lower* panels) of the transitions observed for angiotensinogen, EGF containing fibulin, gelsolin, and prostaglandin D2 synthase. Significant increases ($p < 0.05$) in the expression of angiotensinogen, EGF containing fibulin and gelsolin were observed in patients with respect to healthy subjects, whereas prostaglandin D2 synthase expression decreased significantly ($p < 0.01$) in AS patients with respect to healthy subjects. *In chromatograms: Isobaric or nearly isobaric peptides.

level by the differentiation of mast cells to macrophages (23, 25). The PTX3 protein, which has recently been implicated in innate immunity, is thought to be a marker of vascular inflammation and damage (45, 46). Given that PTX3 is predominantly released by inflamed tissue in response to proinflammatory cytokines (TNF-α and IL-1β) (47) and, considering the recent proposal that AS may be an inflammatory disease, our findings would be consistent with this hypothesis, because PTX3 secretion was increased in AS valves. Secretion of clusterin protein was much lower in AS valves, in agreement with previous findings in ACS plasma (48), which highlights the occurrence of numerous alterations in protein expression common to both atherosclerosis and AS. Clusterin is a glycoprotein whose function remains unclear, although it has been implicated in complement regulation (49), acute phase response (50), lipid transport (51), apoptosis (52), and membrane protection at the tissue-fluid interface where it is expressed.

These data shows a subset of identified proteins differentially expressed in the secretome of AS human valvular tissue with clinical relevance. A further step in the discovery of novel

tools for early diagnostic and prognostic evaluation of AS goes through the possibility to detect physiopathological changes in an easily accessible biological fluid. We evaluated here the variation of the trends of particular proteins in plasma from a wide cohort of patients and healthy subjects, finding gelsolin as a robust potential marker of disease. Gelsolin was found increased both in secretome and plasma AS samples compared with its level in healthy individuals. These data reflect the opposite trend to that found in the secretome from atherosclerotic coronary tissue compared with mammary (control) secretome (13), pointing to clear differences between the mechanisms of atherosclerosis and aortic stenosis. Pathway analysis of labeled proteins (either in control or pathological valves) revealed them as constituents of a network related to "Cellular Movement, Connective Tissue Disorders, Cardiovascular System Development and Function" with maximum significant score. Additionally, cellular movement, assembly and organization, and protein synthesis are functions significantly associated to this set of proteins, pointing to expected mechanisms involved in this pathology.
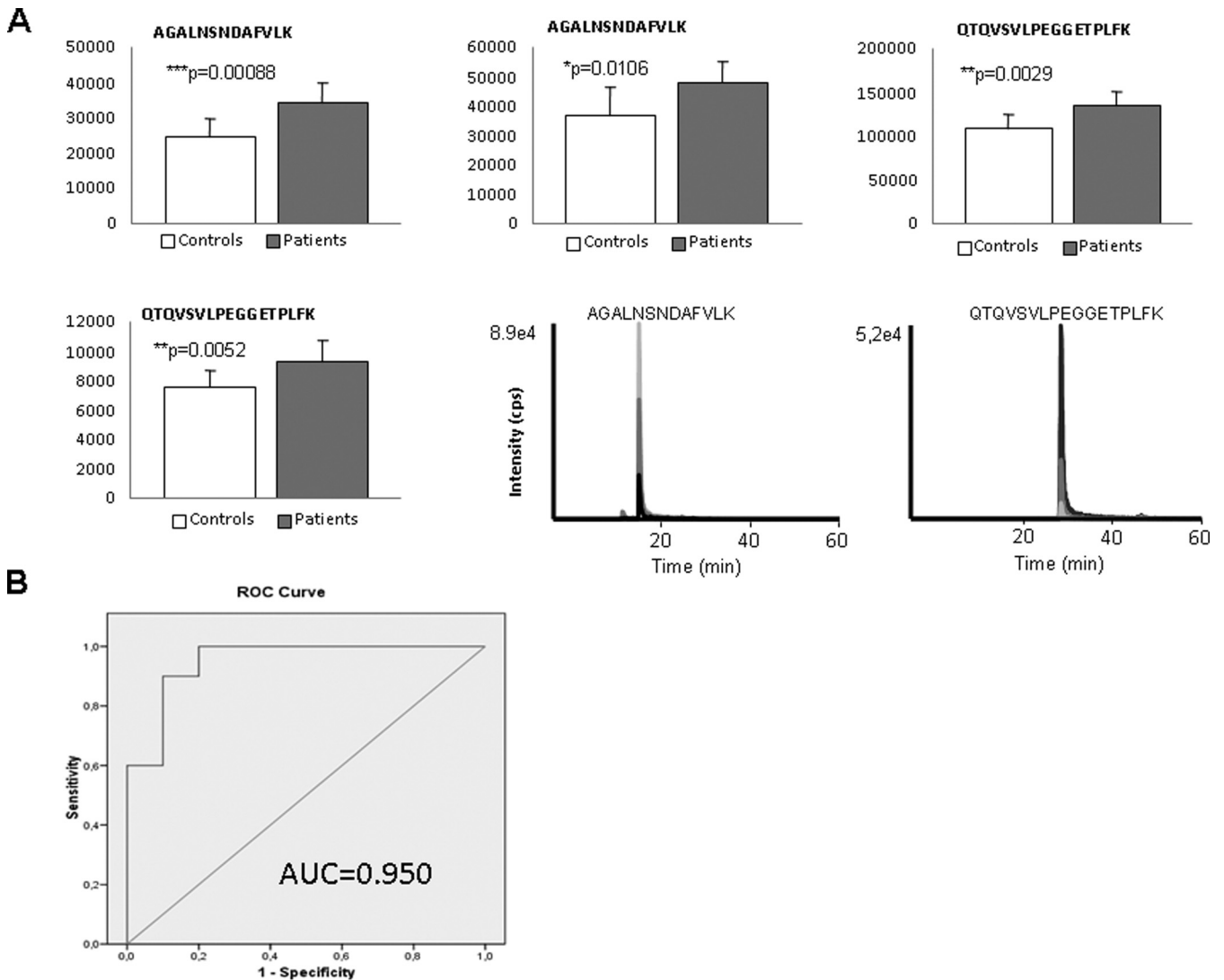
FIG. 6. **SRM results in crude plasma (*n* = 43 patients and *n* = 37 controls) for gelsolin.** *A*, Graphical representation of the abundance and representative extracted ion chromatograms of significant transitions. *B*, ROC curve, calculated with the three significant transitions measured by peptide for a total of two peptides.

In conclusion, our results demonstrate the importance of secretome analysis in aortic stenosis, both to identify new potential biomarkers and to further understand the pathophysiology of this disease. The identification of specific protein secretion patterns altered with disease constitutes valuable information in terms of novel mechanisms of action, and a starting point to further investigate the possibility to act on these proteins through therapy. The use of metabolic labeling unequivocally ensures that all labeled proteins have been secreted or released by aortic valves. Importantly, particular proteins identified are involved in the atherosclerotic process, supporting the emerging hypothesis of a common link between both pathologies. On the other hand, gelsolin has here been demonstrated to be a high sensitivity biomarker of AS, with an opposite trend of secretion to plasma than atherosclerotic arterial tissue (13), which makes it a potential ideal

discriminant biomarker of both pathologies. Our approach also exemplifies the development of specific and sensitive assays to validate biomarkers in the secretome. The proteins differentially secreted during aortic stenosis pathogenesis hereby reported, have been validated by two different techniques (WB and SRM) on an independent group of secretomes. In addition, plasma analyses corroborate the observed variations within the blood pointing to specific candidate markers to follow up in diagnosis, prognosis, and therapeutic intervention.

REFERENCES

1. Cowell, S. J., Newby, D. E., Boon, N. A., and Elder, A. T. (2004) Calcific aortic stenosis: same old story? *Age Ageing* **33,** 538–544

2. Peltier, M., Trojette, M. E., Sarano, M. E., Grigioni, F., Slama, M. A., and Tribouilloy, C. M. (2003) Relation between cardiovascular risk factors and nonrheumatic: severe calcific aortic stenosis among patients with a three-cuspid aortic valve. *Am. J. Cardiol.* **91,** 97–99

3. Pohle, K., Maffort, R., Ropers, D., Moshage, W., Stilianakis, N., Daniel, W. G., and Achenbach, S. (2001) Progression of aortic valve calcification: association with coronary atherosclerosis and cardiovascular risk factors. *Circulation* **104,** 1927–1932

4. Zwickl, H., Traxler, E., Staettner, S., Parzefall, W., Grasl-Kraupp, B., Karner, J., Schulte-Hermann, R., and Gerner, C. (2005) A novel technique to specifically analyze the secretome of cells and tissues. *Electrophoresis* **26,** 2779–2785

5. Tjalsma, H., Antelmann, H., Jongbloed, J. D., Braun, P. G., Darmon, E., Dorenbos, R., Dubois, J. Y., Westers, H., Zanen, G., Quax, W. J., Kuipers, O. P., Bron, S., Hecker, M., and van, Dijl, J. M. (2004) Proteomics of Protein Secretion by Bacillus subtilis: Separating the "secrets" of the Secretome. *Microbiol. Mol. Biol. Rev.* **68,** 207–233

6. Chenau, J., Michelland, S., Sidibe, J., and Seve, M. (2008) Peptides OFFGEL electrophoresis: a suitable pre-analytical step for complex eukaryotic samples fractionation compatible with quantitative iTRAQ labeling. *Proteome Sci.* **26,** 6–9

7. Chan, K. L., Teo, K., Dumesnil, J. G., Ni, A., Tam, J.; ASTRONOMER Investigators (2010) Effect of lipid lowering with rosuvastatin on progression of aortic stenosis: results of the aortic stenosis progression observation: measuring effects of rosuvastatin (ASTRONOMER) trial. *Circulation* **121,** 306–314

8. Chan, K. L., and Teo, K. (2005) Lipid-lowering therapy in calcific aortic stenosis. *N. Engl. J. Med.* **353,** 1066–1067

9. Gil-Dones, F., Darde, V. M., Alonso-Orgaz, S., Lopez-Almodovar, L., Mourino-Alvarez, L., Padial, L. R., Vivanco, F., and Barderas, M. G. (2012) Inside human aortic stenosis: a proteomic profile of plasma. *J. Proteomics* **75,** 1639–1653

10. Martin-Rojas, T., Gil-Dones, F., Lopez-Almodovar, L., Padial, L. R., Vivanco, F., and Barderas, M. G. (2012) Proteomic profile of human aortic stenosis: insights into degenerative process, *J. Proteome Res.* **11,** 1537–1550

11. Hanash, S. M., Pitteri, S. J., and Faca, V. M. (2008) Mining the plasma proteome for cancer biomarkers. *Nature* **452,** 571–579

12. Good, D. M., Thongbookerd, V., Novak, J., Bascands, J. L., Schanstra, J. P., Coon, J. J., Dominiczak, A., and Mischak, H. (2007) Body fluid proteomics for biomarkers discovery: lessons from the past hold the key to succes in the future. *J. Proteome Res.* **6,** 4549–4555

13. de la Cuesta, F., Barderas, M. G., Calvo, E., Zubiri, I., Maroto, A. S., Darde, V. M., Martin-Rojas, T., Gil-Dones, F., Posada-Ayala, M., Tejerina, T., Lopez, J. A., Vivanco, F., and Alvarez-Llamas, G. (2012) Secretome analysis of atherosclerotic and non-atherosclerotic arteries reveals dynamic extracellular remodeling during pathogenesis. *J. Proteomics* **75,** 1639–1653

14. Alvarez-Llamas, G., Szalowska, E., de Vries, M. P., Weening, D., Landman, K., Hoek, A., Wolffenbuttel, B. H., Roelofsen, H., and Vonk, R. J. (2007) Characterization of the human visceral adipose tissue secretome. *Mol. Cell. Proteomics* **6,** 589–600

15. Martin-Ventura, J. L., Duran, M. C., Blanco-Colio, L. M., Meilhac, O., Leclercq, A., Michel, J. B., Jensen, O. N., Hernandez-Merida, S., Tuñón, J., Vivanco, F., and Egido, J. (2004) Identification by a differential proteomic approach of heat shock protein 27 as a potential marker of atherosclerosis. *Circulation* **110,** 2216–2219

16. Bendtsen, J. D., Jensen, L. J., Blom, N., Von, H. G., and Brunak, S. (2004) Feature-based prediction of non classical and leaderless protein secretion. *Protein Eng Des Sel.* **17,** 349–356

17. Berk, B. C., Fujiwara, K., and Lehoux, S. (2007) ECM remodeling in hypertensive heart disease. *J. Clin. Invest.* **117,** 568–575

18. Ballard, V. L., Sharma, A., Duignan, I., Holm, J. M., Chin, A., Choi, R., Hajjar, K. A., Wong, S. C., and Edelberg, J. M. (2006) Vascular tenascin-C regulates cardiac endothelial phenotype and neovascularization *FASEB J.* **20,** 717–719

19. Towbin, J. A., Casey, B., and Belmont, J. (1999) The molecular basis of vascular disorders. *Am. J. Hum. Genet.* **4,** 678–684

20. Kobayashi, N., Kostka, G., Garbe, J. H., Keene, D. R., Bächinger, H. P., Hanisch, F. G., Markova, D., Tsuda, T., Timpl, R., Chu, M. L., and Sasaki, T. (2007) A Comparative Analysis of the Fibulin Protein Family: Biochemical Characterization, Binding Interactions, and Tissue localization. *J. Biol. Chem.* **282,** 11805–11816

21. Kielty, C. M. (2006) Elastic fibres in health and disease. *Expert Rev. Mol. Med.* **8,** 1–23

22. Timpl, R., Sasaki, T., Kostka, G., and Chu, M. L. (2003) Fibulins: a versatile family of extracellular matrix proteins. *Nat. Rev. Mol. Cell Biol.* **4,** 479–489

23. Silacci, P., Mazzolai, L., Gauci, C., Stergiopulos, N., Yin, H. L., and Hayoz, D. (2004) Gelsolin superfamily proteins: key regulators of cellular functions. *Cell Mol. Life Sci.* **61,** 2614–2623

24. Nishio, R., and Matsumori, A. (2009) Gelsolin and cardiac myocyte apoptosis. A new target in the treatment of postinfarction remodeling. *Circulation Res.* **104,** 829–831

25. Lader, A. S., Kwiatkowski, D. J., and Cantiello, H. F. (1999) Role of gelsolin in the actin filament regulation of cardiac L-type calcium channels. *Am. J. Physiol.* **277,** C1277–C1283

26. Yang, J., Moravec, C. S., Sussman, M. A., DiPaola, N. R., Fu, D., Hawthorn, L., Mitchell, C. A., Young, J. B., Francis, G. S., McCarthy, P. M., and Bond, M. (2000) Decreased SLIM1 expression and increased gelsolin expression in failing human hearts measured by high-density oligonucleotide arrays. *Circulation* **102,** 3046–3052

27. Mann, D. L. (2005) Left ventricular size and shape: determinants of mechanical signal transduction pathways. *Heart Fail. Rev.* **10,** 95–100

28. Freeman, R. V., and Otto, C. M. (2005) Spectrum of Calcific Aortic Valve Disease Pathogenesis, Disease Progression, and Treatment Strategies. *Circulation* **111,** 3316–3326

29. Pellieux, C., Desgeorges, A., Pigeon, C. H., Chambaz, C., Yin, H., Hayoz, D., and Silacci, P. (2003) Cap G, a gelsolin family protein modulatin protective effects of unidirectional shear stress. *J. Biol. Chem.* **278,** 29136–29144

30. Silacci, P., Formentin, K., Bouzourène, K., Daniel, F., Brunner, H. R., and Hayoz, D. (2000) Unidirectional and oscillatory shear stress differentially modulate NOS III gene expression. *Nitric Oxide* **4,** 47–56

31. Yang, J., Moravec, C. S., Sussman, M. A., DiPaola, N. R., Fu, D., Hawthorn, L., Mitchell, C. A., Young, J. B., Francis, G. S., McCarthy, P. M., and Bond, M. (2000) Decreased SLIM1 Expression and Increased Gelsolin Expression in Failing Human Hearts Measured by High-Density Oligonucleotide Arrays. *Circulation* **102,** 3046–3052

32. Dawson, D. W., Volpert, O. V., Gillis, P., Crawford, S. E., Xu, H., Benedict, W., and Bouck, N. P. (1999) Bouck NP Pigment epithelium-derived factor: a potent inhibitor of angiogenesis. *Science* **285,** 245–248

33. Duh, E. J., Yang, H. S., Suzuma, I., Miyagi, M., Youngman, E., Mori, K., Katai, M., Yan, L., Suzuma, K., West, K., Davarya, S., Tong, P., Gehlbach, P., Pearlman, J., Crabb, J. W., Aiello, L. P., Campochiaro, P. A., and Zack, D. J. (2002) Pigment epithelium-derived factor suppresses ischemia-induced retinal neovascularization and VEGF-induced migration and growth. *Invest. Ophthalmol. Vis. Sci.* **43,** 821–829

34. Yamagishi, S., Adachi, H., Abe, A., Yashiro, T., Enomoto, M., Furuki, K.,

Hino, A., Jinnouchi, Y., Takenaka, K., Matsui, T., Nakamura, K., and Imaizumi, T. (2006) Elevated serum levels of pigment epithelium-derived factor in the metabolic syndrome. *J. Clin. Endocrinol. Metab.* **91,** 2447–2450

35. Zelko, I. N., Mariani, T. J., and Folz, R. J. (2002) Superoxide dismutase multigene family: a comparison of the CuZn-SOD (SOD1), Mn-SOD (SOD2) and EC-SOD (SOD3) gene structures, evolution and expression. *Free Radic. Biol. Med.* **33,** 337–349

36. Miura, T., Nishina, T., and Terada, T. (2008) Different functions between human monomeric carbonyl reductase 3 and carbonyl resductase 1. *Mol. Cell. Biochem.* **315,** 113–121

37. Ellis, E. M. (2007) Reactive carbonyls and oxidative strees: potential for therapeutic intervention. *Pharmacol. Ther.* **115,** 13–24

38. Bagnato, C., Thumar, J., Mayya, V., Hwang, S. I., Zebroski, H., Claffey, K. P., Haudenschild, C., Eng, J. K., Lundgren, D. H., and Han, D. K. (2007) Proteomics analysis of human coronary atherosclerotic plaque: a feasibility study of direct tissue proteomics by liquid chromatography and tandem mass spectrometry. *Mol. Cell. Proteomics* **6,** 1088–1102

39. Berg, A. H., and Scherer, P. E. (2005) Adipose Tissue, Inflammation, and Cardiovascular Disease. *Circ. Res.* **96,** 939–949

40. Schieffer, B., Bunte, C., Witte, J., Hoeper, K., Böger, R. H., Schwedhelm, E., and Drexler, H. (2004) Comparative effects of AT1-antagonism and angiotensin converting enzyme inhibition on markers of inflammation and platelet aggregation in patients with coronary artery disease. *J. Am. Coll. Cardiol.* **44,** 362–368

41. DeLany, J. P., Floyd, Z. E., Zvonic, S., Smith, A., Gravois, A., Reiners, E., Wu, X., Kilroy, G., Lefevre, M., and Gimble, J. M. (2005) Secretome of primary cultures of human adipose-derived stem cells. *Mol. Cell. Proteomics* **4,** 731–740

42. Giles, H., and Leff, P. (1988) The biology and pharmacology of PGD2. *Prostaglandins* **35,** 277–300

43. Eguchi, Y., Eguchi, N., Oda, H., Seiki, K., Kijima, Y., Matsu-ura, Y., Urade, Y., and Hayaishi, O. (1997) Expression of lipocalin-type prostaglandin D synthase (b-trace) in human heart and its accumulation in the coronary circulation of angina patients. *Proc. Natl. Acad. Sci.* **94,** 14689–14694

44. Urade, Y., and Hayaishi, O. (2000) Biochemical, structural, genetic, physiological, and pathophysiological features of lipocalin-type prostaglandin D synthase. *Biochim. Biophys. Acta* **1482,** 259–271

45. Wolf-Yadlin, A., Hautaniemi, S., Lauffenburger, D. A., and Hite, F. M. (2007) Multiple reaction monitoring for robust quantitative proteomic analysis of cellular signaling networks. *Proc. Natl. Acad. Sci. U.S.A.* **104,** 5860–5865

46. Mantovani, A., Garlanda, C., Bottazzi, B., Peri, G., Doni, A., Martinez de la Torre, Y., and Latini, R. (2006) The long pentraxin PTX3 in vascular pathology. *Vascul. Pharmacol.* **45,** 326–330

47. Jenny, N. S., Arnold, A. M., Kuller, L. H., Tracy, R. P., and Psaty, B. M. (2009) Associations of Pentraxin 3 with cardiovascular disease and all-cause death. The Cardiovascular Health Study. *Arterioscler. Thromb. Vasc. Biol.* **29,** 594–599

48. Darde, V. M., de la Cuesta, F., Gil-Dones, F., Alvarez-Llamas, G., Barderas, M. G., and Vivanco, F. (2010) Analysis of the plasma proteome associated with acute coronary síndrome. Does a permanet protein signature exist in the plasma of ACS patients? *J. Proteome Res.* **9,** 4420–4432

49. Tschopp, J., Chonn, A., Hertig, S., and French, L. E. (1993) Clusterin, the human apolipoprotein and complement inhibitor, binds to complement C7, C8 beta, and the b domain of C9. *J. Immunol.* **151,** 2159–2165

50. Hardardóttir, I., Kunitake, S. T., Moser, A. H., Doerrler, W. T., Rapp, J. H., Grünfeld, C., and Feingold, K. R. (1994) Endotoxin and cytokines increase hepatic messenger RNA levels and serum concentrations of apolipoprotein J (clusterin) in Syrian hamsters. *J. Clin. Invest.* **94,** 1304–1309

51. Rosenberg, M. E., and Silkensen J. (1995) Clusterin: physiologic and pathophysiologic considerations. *Int. J. Biochem. Cell Biol.* **27,** 633–645

52. O'Sullivan, J., Whyte, L., Drake, J., and Tenniswood, M. (2003) Alterations in the post-translational modification and intracellular trafficking of clusterin in MCF-7 cells during apoptosis. *Cell Death Differ.* **10,** 914–927